*Thermochimica Acta*, 113 (1987) 359–368
Elsevier Science Publishers B.V., Amsterdam – Printed in The Netherlands

# DETERMINATION OF PHASE STABILITY IN THE Sr–S–O SYSTEM

Z. PANEK and K. FITZNER

*Institute for Metals Research, Polish Academy of Science, 25 Reymonta Street, 30-059 Kraków (Poland)*

(Received 18 August 1986)

## ABSTRACT

By means of the following solid oxide galvanic cells:

$\mathrm{Pt,Ni + NiO}\,|\,\mathrm{O^{2-}}\,|\,\mathrm{SrSO_4 + SrS,Au}$

and

$\mathrm{Pt,Fe + FeO}\,|\,\mathrm{O^{2-}}\,|\,\mathrm{SrSO_4 + SrO,Au}$

the equilibrium oxygen pressure was determined for the reactions

$\mathrm{SrS + 2\,O_2 \rightarrow SrSO_4}$

and

$\mathrm{SrSO_4 \rightarrow SrO + SO_2 + \frac{1}{2}O_2}$

Results obtained under "closed cell" conditions suggest that the Gibbs free energy change for the reaction of sulphate decomposition into SrO and the gas phase is much lower than that reported in thermochemical tables. For this reaction, experiments yielded

$\Delta G_T^0 = 882550 - 438.3T\ \mathrm{J\ mol^{-1}}$

in the temperature range 973–1273 K.

Conditions of phase equilibria for the Sr–S–O system at 1273 K were suggested, and kinetics of the reduction reaction

$\mathrm{SrSO_4 + 4\,H_2 \rightarrow SrS + 4\,H_2O}$

were investigated in the temperature range 1073–1273 K.

## INTRODUCTION

Strontium and its compounds find numerous applications in modern technology. Strontium carbonate is used in the electronics industry for TV screen production. Al–Si alloys with 10 wt% Sr addition are used to influence the structure of Al alloys during casting. Strontium sulphide, due to its high thermodynamic stability and NaCl-type structure, is a potential candidate as a solid electrolyte conducting either with sulphur or strontium ions.

Since Polish sulphur deposits occur in strontium sulphate beds, it is interesting to consider conditions of equilibrium among different strontium compounds, and to determine the range of stability of strontium sulphate. A number of investigations of sulphate decomposition reactions were carried out by Skeaff and Espelund [1], who used a solid-state EMF technique; however, none of these concerned $SrSO_4$. Recently, Fredriksson and Rosén [2] performed thermodynamic studies of high-temperature equilibria between SrS and $SrSO_4$ using solid-state EMF measurements. A similar experimental method was also used in the present study.

## EXPERIMENTAL

### *Materials*

Strontium sulphate was obtained by precipitation from an $SrCl_2$–water solution acidified with $H_2SO_4$. Strontium chloride was obtained from Reachim (U.S.S.R.) and was 99.7% pure. A mixture of $SrSO_4$ and SrS powders was produced by partial $SrSO_4$ reduction under flowing hydrogen at 1073 K for 6 h. Strontium oxide (SrO) was obtained by $Sr(NO_3)_2$ decomposition at 1373 K in air. Strontium nitrate was obtained from Polskie Odczynniki Chemiczne, Gliwice (Poland), and was reagent grade.

Nickel and nickel oxide (both 99.95% pure), used for the reference electrode, were obtained from International Nickel Ltd. and BDH, respectively. The Fe + FeO reference electrode was prepared by mixing Fe and $Fe_2O_3$ powders at 3 : 1 molar ratio. Powders of Fe and $Fe_2O_3$ were obtained from Johnson Matthey Chemicals Ltd. (U.K.) and from Merck (F.R.G.), and were 99.99 and 99.95% pure, respectively. CSZ tubes, closed at one end, were supplied by Degussa (F.R.G.).

### *Oxygen potential measurements*

#### *$SrS$–$SrSO_4$ equilibrium*

An EMF cell of the type

$$\mathrm{Pt,Ni + NiO\,|\,ZrO_2 + CaO\,|\,SrS + SrSO_4,Au} \qquad \text{(I)}$$

was used for oxygen potential measurements. The equilibrium oxygen pressure of the reaction

$$\mathrm{SrS + 2\ O_2 \rightarrow SrSO_4} \qquad (1)$$

is directly related to the EMF of cell (I) by the relationship

$$\ln p_{O_2} = \left(2\ \Delta G^0_{f,NiO} - 4FE_I\right)/RT \qquad (2)$$

where $F = 23063$ cal V mol$^{-1}$, $E$ is the EMF in volts, $R$ is the gas constant,

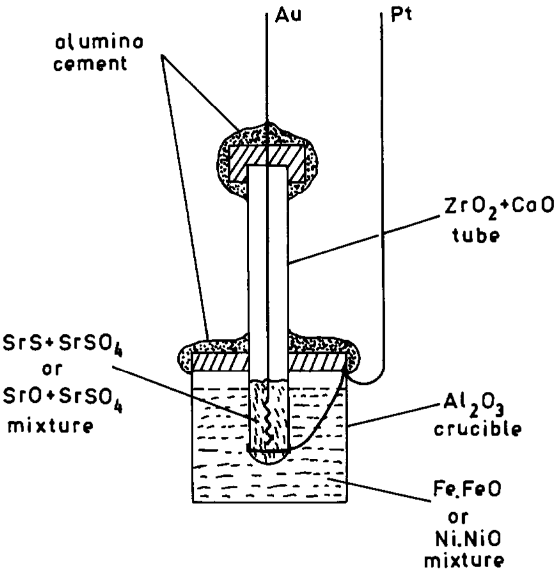

Fig. 1. Schematic diagram of the cell assembly.

and $T$ is the absolute temperature. The Gibbs free energy of formation of nickel oxide, $\Delta G^0_{f,NiO}$, was taken from Steele [3].

A schematic diagram of the cell assembly is shown in Fig. 1. A solid electrolyte tube was inserted into an alumina crucible filled with Ni + NiO powder, and the tube was tightly wound with platinum wire from outside. $SrSO_4$ + SrS powder was sealed inside the CSZ tube with an alumina cement and the gold wire which made a conducting lead to the cell. The cell was kept in the constant temperature zone of a resistant furnace under a stream of pure argon. Copper chips were used as a getter to maintain the desired oxygen pressure in the gas phase.

After constant temperature had been reached the cell was left for 24 h to attain equilibrium. Then, the EMF was recorded by means of a V 534 digital voltmeter (Elwro, Poland). The cell operated reversibly for four days.

The results of EMF measurements produced by cell (I), after necessary thermo-EMF Pt-Au corrections, are shown in Fig. 2. The Pt–Au thermo-EMF was measured separately and is shown in Fig. 3. Using the least-squares method the temperature dependence of EMFs was described with the following equation:

$$E_I = 52.35 - 6.042 \times 10^{-3} T \text{ (mV)} \quad (3)$$

and consequently, equilibrium oxygen pressure of reaction (1):

$$\log p_{O_2} = -25520/T + 8.99 \quad (4)$$

was derived from eqn. (2).

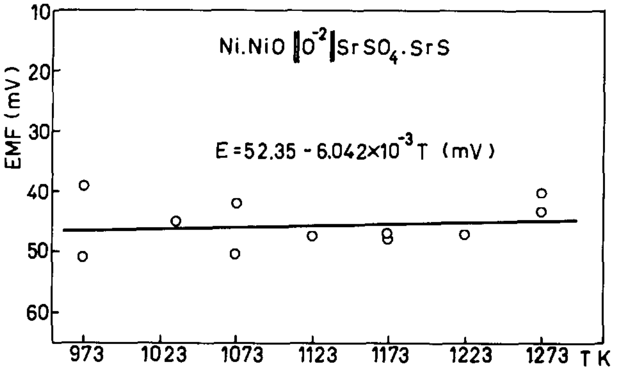

Fig. 2. Temperature dependence of the EMF of cell I.

Values of log $p_{O_2}$ calculated from eqn. (4) are compared in Fig. 4 with results derived from EMF measurements by Fredriksson and Rosén [2]. Good agreement was found which demonstrated that the closed cell construction applied in this work was gas-tight enough to produce a reliable equilibrium oxygen pressure in the metal sulphide–metal sulphate system.

*SrO–SrSO$_4$ equilibrium*

Again, the EMF measurements were carried out using a closed cell construction. Judging from the experiments on SrS–SrSO$_4$ equilibria, the

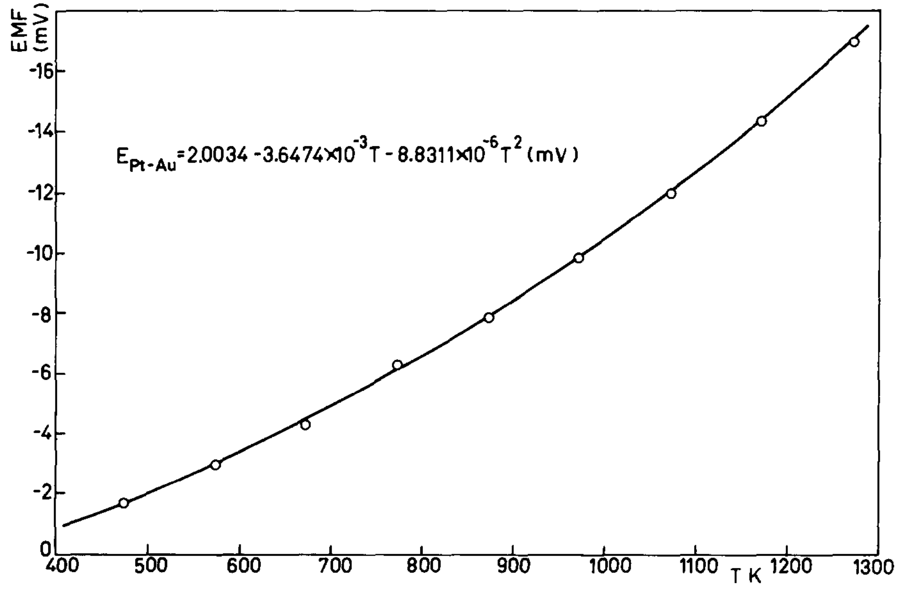

Fig. 3. Pt–Au thermo-EMFs vs. temperature.

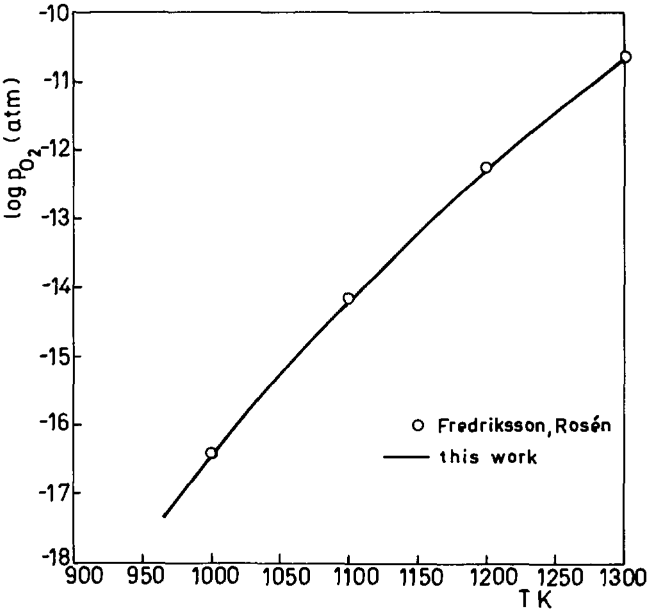

Fig. 4. Values of log $p_{O_2}$ vs. temperature obtained in this work (———) and from ref. 2 (○).

seal was tight enough to maintain the composition of the gas phase corresponding to the equilibrium of the decomposition reaction

$$SrSO_4 \rightarrow SrO + SO_2 + \tfrac{1}{2} O_2 \tag{5}$$

Since the whole cell remained within the constant temperature zone of the furnace, the influence of thermal diffusion on the composition of the gas should be eliminated. Under the above conditions

$$p_{SO_2} = 2\ p_{O_2} \tag{6}$$

and assuming that there is no mutual solubility between SrO and $SrSO_4$, the equilibrium constant of reaction (5) can be expressed as follows:

$$K_{(5)} = p_{SO_2} p_{O_2}^{1/2} = 2 p_{O_2}^{3/2} \tag{7}$$

At a fixed temperature the oxygen potential can be determined from EMF values of the cell

$$Pt,Fe + FeO\,|\,ZrO_2 + CaO\,|\,SrO + SrSO_4,Au \tag{II}$$

which corresponds to the equilibrium oxygen pressure over the SrO + $SrSO_4$ mixture through the relation

$$\ln p_{O_2} = \left(2\Delta G^0_{f,FeO} - 4FE_{II}\right)/RT \tag{8}$$

EMFs produced by cell (II) are shown in Fig. 5 after necessary thermo-EMF

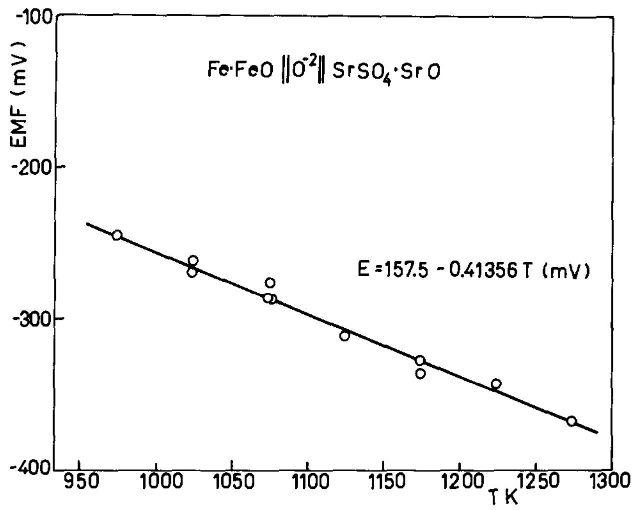

Fig. 5. Temperature dependence of the EMF of cell II.

corrections. Using the least-squares method the temperature dependence was obtained in the form

$$E_{II} = 157.5 - 0.41356T \text{ (mV)} \qquad (9)$$

If the Gibbs free energy of FeO formation is taken from Turkdogan [4], the equilibrium oxygen pressure calculated from eqn. (8) is

$$\log p_{O_2} = -30730/T + 15.06 \qquad (10)$$

and, consequently, the Gibbs free energy change of reaction (5) can be calculated from the relation

$$\Delta G_T^0 = -RT \ln K_{(5)} = -RT \ln\left(2p_{O_2}^{3/2}\right) = 882550 - 438.3T \text{ (J mol}^{-1}\text{)} \qquad (11)$$

Equation (11) yields free energy values much lower than those reported in thermochemical tables [4].

## PHASE EQUILIBRIA AT 1273 K

Metallic (Sr), oxide (SrO), sulphide (SrS) and sulphate ($SrSO_4$) phases occur in the Sr–S–O system, which can exist in equilibrium with the $S_2$–$O_2$ gas phase. Calculations showed that the reaction

$$Sr + SrSO_4 \rightarrow SrO + SO_2 \qquad (12)$$

would proceed spontaneously to the right and, consequently, the composition diagram for the Sr–S–O system at 1273 K should reveal three fields of stability corresponding to three condensed phases as presented in Fig. 6b.

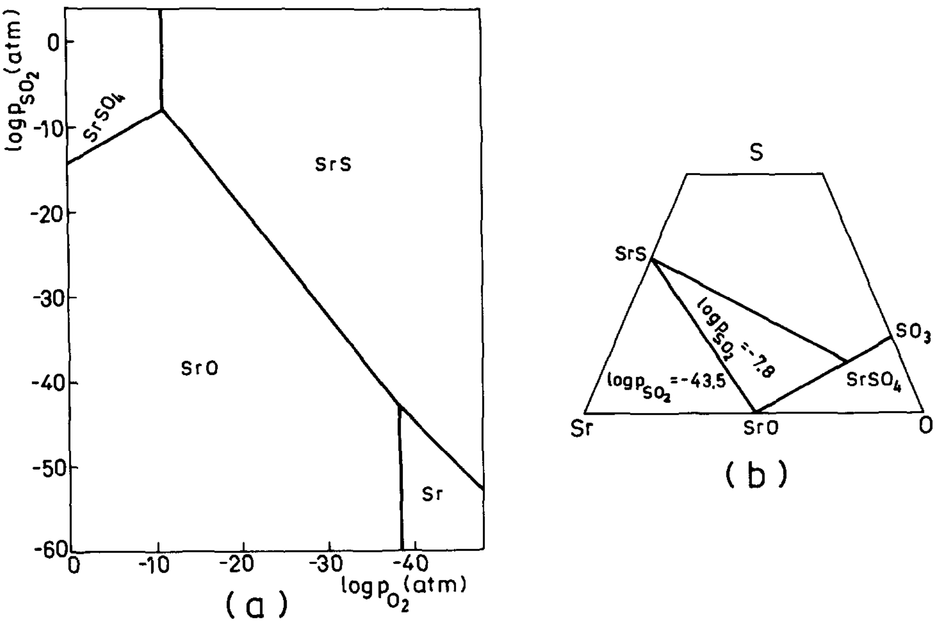

Fig. 6. Stability diagram of the Sr–S–O system at $T = 1273$ K.

Bivariant equilibria in the Sr–S–O system, involving two condensed phases and the gas phase ($O_2$ and $SO_2$ are chosen as the variable parameters), are shown in Fig. 6a. Intersections of three bivariant equilibria correspond to one of the univariant equilibria shown in Fig. 6b. The areas between bivariant lines represent regions of stability of a single condensed phase.

The thermodynamic data used for the calculations were taken from published tables [4], except those for reactions (1) and (5) which were determined in this study. The bivariant line corresponding to the reaction

$$SrS + \tfrac{3}{2}\ O_2 \rightarrow SrO + SO_2 \tag{13}$$

was drawn as a compromise between univariant points calculated from our data ($SrSO_4$–SrO–SrS) and from the tables (Sr–SrO–SrS) [4]. Generally, the literature data for sulphide and sulphate may be uncertain.

## KINETICS OF $SrSO_4$ REDUCTION WITH HYDROGEN

Kinetics of $SrSO_4$ reduction with hydrogen according to the reaction

$$SrSO_4 + 4\ H_2 \rightarrow SrS + 4\ H_2O \tag{14}$$

were also studied.

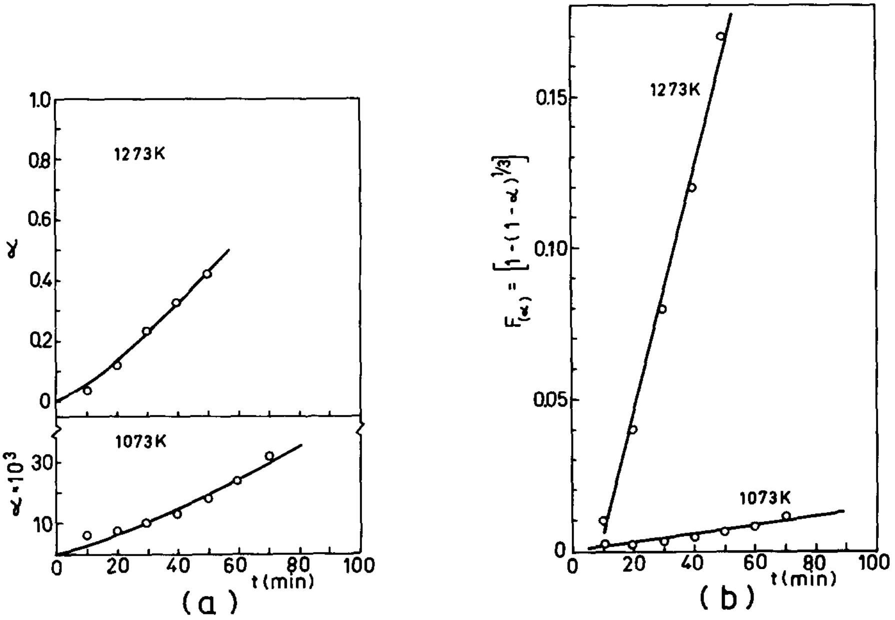

Fig. 7. Results of weight loss experiments for reaction (14).

The material used in this experiment was $SrSO_4$ powder, which was dried at ca. 400 K before use. The reduction of the sample took place in the vertical furnace tube of a TA-1 Mettler thermobalance. At first, just an alumina crucible was suspended in the furnace and fired at 1273 K. Virtually no weight change was observed. Next, the experiment was run under flowing argon. After the required temperature had been reached, again virtually no weight loss of the $SrSO_4$ sample was detected. During the temperature increase, however, a slight weight change of the sample was recorded. Thus, for further experiments the weight $m(t = 0)$ was accepted for the situation when the required temperature had been reached under argon, and the gas atmosphere was then changed to pure hydrogen.

The time record was started when the first weight change was detected after admission of the reducing atmosphere. The weight loss of the sample was automatically recorded during the process of reduction. Tests were made for two temperatures (1073 and 1273 K) and the results are shown with circles in Fig. 7a.

Kinetically, it is reasonable to consider $SrSO_4$ in the process of reduction as a single two-phase system: sulphate/sulphide. However, we stress that we do not intend to suggest any physical model for this process. Our aim was to develop a formal description of the experimental data in order to establish time–temperature conditions for the entire conversion of $SrSO_4$ into SrS. For this purpose the equation suggested by McKewan [5], who investigated the kinetics of iron oxide reduction, was adopted. This rate equation has the form

$$F(\alpha) = 1 - (1 - \alpha)^{1/3} = kt \tag{15}$$

where $\alpha$ is the fractional reduction defined as the weight of oxygen removed divided by the total weight of oxygen originally present in the sample: $\alpha = [m(t=0) - m(t)]/m(t=0)$; $k$ is a function of temperature; and $t$ is time.

The corresponding dependence of $F(\alpha)$ vs. time is shown in Fig. 7b. A linear plot was obtained with values of $k$ equal to $1.5 \times 10^{-4}$ and $4 \times 10^{-3}$ at 1073 and 1273 K, respectively. Experimental data can be reproduced by eqn. (15) (solid line in Fig. 7a) if a small shift of the curve is introduced, since $F(\alpha)$ vs. $t$ plots do not pass through the origin. The corrected eqn. (15) takes the form

$$F(\alpha) = f(T) + kt \tag{16}$$

with $f(T) = -5 \times 10^{-3}$ and $-36 \times 10^{-3}$ at 1073 and 1273 K, respectively. From these equations, a time of 4.3 h was derived for complete conversion of $SrSO_4$ into SrS under hydrogen at 1273 K.

## DISCUSSION

The most striking feature of the results is the large discrepancy in $\Delta G_T^0$ for reaction (5). Agreement with the results of Fredriksson and Rosén was achieved for reaction (1), indicating that satisfactory “closed cell” conditions were provided by the construction of the cell. The whole cell remained within the constant temperature zone of the furnace and no thermal gradient appeared along the electrolyte tube. Thus, the gas phase inside the tube should be uniform due to the lack of thermal diffusion. High $SrSO_4$ stability and a subsequent low decomposition pressure should help to achieve equilibrium inside the tube.

However, it is still possible that there was a steady exchange of gas through the alumina cement, and the “closed cell” condition was violated. Moreover, possible traces of $Sr(NO_3)_2$, left after firing during SrO production, could affect the gas composition inside the tube by changing the equilibrium oxygen pressure. In order to resolve this controversy, investigations should be repeated in another laboratory with materials of higher purity. Careful analysis of the thermochemical data in published tables for $SrSO_4$ revealed that in fact reliable $c_p$ measurements for this compound do not exist.

The results obtained helped in the construction of a stability diagram for the Sr–S–O system. The condition of conversion of one phase into another are explained to a certain extent. From our point of view the most interesting compound is SrS: it is the basis for the production of soluble inorganic strontium compounds; it exhibits very high thermodynamic stability and at the same time its electrical conductivity and structure make it a potential candidate for solid electrolytes conducting either with $Sr^{2+}$ or with $Sr^{2-}$ ions [6]. Thus, the kinetics of $SrSO_4$ reduction were also studied. In principle this process can be controlled by three steps:

(1) gas transfer to and from the bulk gas stream,
(2) diffusion of the reactant and product gases across the solid porous layer, and
(3) chemical reaction at the interface.

One may expect that factors (2) and (3) are responsible for this mixed-control process. However, with insufficient information about these mechanisms, the formal description was chosen.

## REFERENCES

1 J.M. Skeaff and A.W. Espelund, Can. Met. Quart., 4 (1973) 445.
2 M. Fredriksson and E. Rosén, Chem. Scr., 16 (1980) 34.
3 C.B.H. Steele, in C.B. Alcock (Ed.), Electromotive Force Measurements in High Temperature Systems, The Institution of Mining and Metallurgy, London, 1968.
4 E.T. Turkdogan, Physical Chemistry of High Temperature Technology, Academic Press, London, 1980.
5 W.M. McKewan, Trans. Met. Soc. AIME, 218 (1960) 2.
6 H. Nakamura, Y. Ogawa, K. Gunji and A. Kasahara, Trans. Jpn. Inst. Met., 25 (1984) 692.